Derivation of an inter-cluster potential from a two-fermion contact interaction

JK

(Dated: June 3, 2020)

Abstract

The potential acting between a point particle and a bound state of A particles is related to the interaction between single particles. Specifically, the A-particle state is totally symmetric in coordinate space ("bosonic"), and the single particles should be amenable to a first-order description with two- and three-body contact/zero-range interactions. Furthermore, the internal space of the $A+1$ equal-mass particles is given as A-dimensional, which demands an $A+1$ body state of mixed symmetry.

4 *a. The inter-cluster potential* In order to study the large-N limit, we develop a model inspired by the resonating-
5 group formalism ([1],[2]). That entails the assumption of a frozen A-body core whose spatially symmetric wave
6 function we parametrize with a single parameter a via

$$\phi_A := e^{-\alpha \sum_{i=1}^A (\boldsymbol{r}_i - \boldsymbol{R}_A)^2} \quad ; \quad \begin{matrix} \boldsymbol{r}_i & : \text{single-particle coordinates} \\ \boldsymbol{R}_A & : \text{core centre of mass} \end{matrix} \quad . \tag{1}$$

7 The system is thereby reduced to only three degrees of freedom, namely the relative distance between core and the
8 odd particle. The respective equation of motion reads in terms of the effective mass μ, the relative kinetic energy E
9 between core and odd particle:

$$\int \left\{ \phi_A^* \left(-\frac{\hbar^2}{2\mu} \boldsymbol{\Delta}_R - E + \mathcal{V} \right) \mathcal{A} \left[\phi_A \psi(\boldsymbol{R}) \right] \right\} d\boldsymbol{r}_{1...A} = 0 \quad . \tag{2}$$

Antisymmetrization is required between two particles only, $\mathcal{A} = \mathbb{1} - P_{A,A+1}$, and the interaction is effective, only if it involves the odd particle:

$$\mathcal{V} = C_0(\Lambda) \sum_i^{A-1} \delta_\Lambda^{(3)} (\boldsymbol{r}_i - \boldsymbol{r}_{A+1}) \tag{3}$$

$$+ D_1(\Lambda) \sum_{i<j}^{A-1} \left[\delta_\Lambda^{(3)} (\boldsymbol{r}_i - \boldsymbol{r}_j) \, \delta_\Lambda^{(3)} (\boldsymbol{r}_i - \boldsymbol{r}_{A+1}) \right. \tag{4}$$

$$\left. + \delta_\Lambda^{(3)} (\boldsymbol{r}_i - \boldsymbol{r}_{A+1}) \, \delta_\Lambda^{(3)} (\boldsymbol{r}_j - \boldsymbol{r}_{A+1}) \right] \quad . \tag{5}$$

10 The contribution from the identical copy of the $(A+1)^{\text{th}}$ particle – without loss of generality identified with label A
11 – interacting is excluded, because we anticipate its vanishing because of antisymmetrization. This *a priori* exclusion
12 introduces artefacts because the zero-range contact forces are approximated via

$$\delta^{(1)}(x) = \lim_{\Lambda \to \infty} \frac{\Lambda}{2\sqrt{\pi}} \cdot e^{-\frac{\Lambda^2}{4} x^2} \tag{6}$$

13 in our calculations in order to obtain regular solutions – in contrast to, *e.g.*, Bethe-Peierls [3] boundary conditions.
14 We assume that those are insignificant relative to the other terms from the inter-fragment interaction.
15   The integration in (2) yields a three-dimensional Schrödinger equation with a non-local potential

$$\left(-\frac{\hbar^2}{2\mu} \boldsymbol{\Delta}_R - E \right) \psi(\boldsymbol{R}) + \sum_{n=1}^3 \eta_n \, e^{-\kappa_n \boldsymbol{R}^2} \psi(\boldsymbol{R}) - \sum_{n=1}^4 \zeta_n \int \left\{ \widehat{\mathfrak{D}}_n e^{-\alpha_n \boldsymbol{R}^2 - \beta_n \boldsymbol{R} \cdot \boldsymbol{R}' - \gamma_n \boldsymbol{R}'^2} \right\} \psi(\boldsymbol{R}') d\boldsymbol{R}' = 0 \quad . \tag{7}$$

The coefficients $\alpha, \ldots, \kappa$ are functions of the number of core particles A, the core size a, the interaction regulator Λ, and the single-particle mass m, and

$$\widehat{\mathfrak{D}}_1 = -\frac{\hbar^2}{2\mu} \boldsymbol{\Delta}_R - E \tag{8}$$

$$\rightarrow -\frac{\hbar^2}{2\mu} \left(4\alpha_1^2 \boldsymbol{R}^2 + \beta_1^2 \boldsymbol{R}'^2 + 4\alpha_1 \beta_1 \boldsymbol{R} \cdot \boldsymbol{R}' - 2\alpha_1 \right) - E \quad ,$$

16 while $\widehat{\mathfrak{D}}_{2,3,4} = \mathbb{1}$. The sign (+) of the first sum – the direct interaction – is that of the microscopic LEC. In contrast,
17 the second, non-local part reverts the sign. For example, the effect of an attractive 2-body potential becomes a
18 repulsive contribution due to antisymmetrization in this term.
19   A few comments are in order. Firstly, $\zeta_{1...4} = 0$ if $\mathcal{A} = \mathbb{1}$, *i.e.*, the inter-cluster potential is local. The first
20 non-local term encodes the so-called exchange interaction. It is non-zero even in the absence of inter-particle forces.

21 The two- and three-body contact forces affect the inter-cluster potential structurally in the same way. However, the
22 respective coefficients differ significantly in their dependence on A, a and Λ. It is the combination of both, the two-
23 and three-body terms, which results in the changing character of the interaction, the formation of attractive and
24 repulsive regions, and thereby the possibility to bind the odd particle to the core. We postpone a detailed analysis of
25 the sensitivity of the inter-cluster potential, for now, and continue with the discussion of the emerging spectrum of
26 (7).

27   b.   *Partial-wave projection*   We solve Eq.(7) by expanding the total wave function[1]

$$\psi(\mathbf{R}) = R^{-1} \sum_{lm} \phi_{lm}(R) Y_{lm}(\hat{\mathbf{R}}) \tag{9}$$

28 and a projection with the integral operator

$$\int d^2\hat{\mathbf{R}} \, Y_{lm}^*(\hat{\mathbf{R}}) \tag{10}$$

29 from the left. The uncoupling of different partial waves becomes explicit when

$$e^{-\beta \mathbf{R} \cdot \mathbf{R}'} = 4\pi \sum_{LM} i^L j_L(i\beta RR') Y_{LM}^*(\hat{\mathbf{R}}) Y_{LM}(\hat{\mathbf{R}}') \tag{11}$$

30 is substituted[2]. In the $n = 1$ part, which encodes the exchange effect on the free Hamiltonian, we apply the Laplacian
31 before making the above and following substitutions:

$$\mathbf{R} \cdot \mathbf{R}' = -\sqrt{3} \left[\mathbf{R}_p \otimes \mathbf{R}'_{-p} \right]^{00} \tag{12}$$

32 with $\mathbf{r}_m = \sqrt{\frac{4\pi}{3}} r Y_{1,m}(\hat{\mathbf{r}})$. Using Eq.(4.6.3) and Eq.(3.7.8) of [4], we obtain the equation of motion for a single partial
33 wave:

$$\left(\frac{\hbar^2}{2\mu} \left[-\partial_R^2 + \frac{l(l+1)}{R^2} \right] - E \right) \phi_{lm}(R) \tag{13a}$$

$$-(-E) \int \left(4\pi \, i^l \cdot \zeta_1 \cdot j_l(i\beta_1 RR') \right) \cdot e^{-\alpha_1 \mathbf{R}^2 - \gamma_1 \mathbf{R}'^2} \phi_{lm}(R') \, RR' dR' \tag{13b}$$

$$-\left(\frac{\hbar^2}{2\mu} \right) \int (4\pi \cdot \zeta_1) \cdot e^{-\alpha_1 \mathbf{R}^2 - \gamma_1 \mathbf{R}'^2} \cdot \left\{ \left[-(4\alpha_1^2 R^2 + \beta_1^2 R'^2 - 2\alpha_1) + \frac{l(l+1)}{R^2} \right] i^l j_l(i\beta_1 RR') \right.$$

$$\left. +(4\alpha_1\beta_1) \cdot RR' \cdot \left(i^{l-1} j_{l-1}(i\beta_1 RR')(2l-3) \begin{pmatrix} 1 & l-1 & l \\ 0 & 0 & 0 \end{pmatrix}^2 + i^{l+1} j_{l+1}(i\beta_1 RR')(2l-1) \begin{pmatrix} 1 & l+1 & l \\ 0 & 0 & 0 \end{pmatrix}^2 \right) \right\} \phi_{lm}(R') \, RR' dR' \tag{13c}$$

$$-\sum_{n=2}^{4} \zeta_n \int (4\pi \, i^l) \cdot j_l(i\beta_n RR') \cdot e^{-\alpha_n \mathbf{R}^2 - \gamma_n \mathbf{R}'^2} \, \phi_{lm}(R') \, RR' \, dR' \tag{13d}$$

$$+\sum_{n=1}^{3} \eta_n \, e^{-\kappa_n \mathbf{R}^2} \phi_{lm}(R) \tag{13e}$$

$$= 0 \quad \text{, with } [\eta_i] = \text{MeV} \quad [\zeta_i] = \text{fm}^{-3}$$

34 This equation defines a generalized Eigenvalue problem

$$\int dR' \, \hat{\mathcal{D}}_{RR'} \, \phi_{lm}(R') = E \int dR' \left(\delta_{RR'} + \hat{\mathcal{K}}_{RR'} \right) \phi_{lm}(R') \tag{14}$$

35 whose solution we expand in a finite set of harmonic oscillator functions[3].

36   c.   *The low-energy ("S-wave") limit*   As a special case, the structure for the $l = 0$ partial wave is detailed below.
37 In virtue of $j_l(i\beta_1 RR') =$

---

[1] Dimensionality: $[\psi] = \text{fm}^{-\frac{3}{2}}$, $[\phi] = \text{fm}^{-\frac{1}{2}}$

[2] See Ref. [4] Eq.(5.8.3) with spherical Bessel functions $j_0(z) = z^{-1} \sin z = \text{sinc } z$.

[3] $\phi_{nl\nu}(R) = N_{nl\nu} R^{l+1} e^{-\nu R^2} L_n^{l+1/2}(2\nu R^2)$ in terms of a normalizing constant $N_{nl\nu} = \left(\left(\frac{2\nu^3}{\pi} \right)^{1/2} \cdot \frac{2^{2l+n+3} n! \nu^l}{(2n+2l+1)!!} \right)^{1/2}$ and generalized
Laguerre polynomials $L_n^m(x)$.

₃₈ *d. Example: dimer-dimer scattering – 2-component Fermions* The scattering of two identical dimers, each com-
₃₉ prised of equal-mass particles which interact resonantly (scattering length significantly larger than the effective range
₄₀ $a^{-1}r \to 0$), at an energy sufficiently low such that the effects of branch cuts due to dimer disintegration and excitation
₄₁ can be neglected, shall serve as a benchmark. For this experiment, the remarkable result

$$\frac{a_{dd}}{a} \approx 0.6 \tag{15}$$

₄₂ for the ratio between S-wave scattering lengths of the dimer-dimer amplitude a_{dd} and the resonant two-fermion system
₄₃ a has been found[5] in a four-body calculation. We use this result as a standard in order to demonstrate the accuracy
₄₄ of the RGM approximation, *i.e.*, the reformulation of the dimer-dimer problem as a two-body system, as well as that
₄₅ of the numerical solution of the ensuing non-local equation.

Pertinent to this system are the following quantities:

$$A = 4 \quad , \quad \mu = m \text{ (single-particle mass)} \quad , \frac{\hbar^2}{2\mu} \overset{\text{nuclear}}{=} 20.7 \text{ MeV} \cdot \text{fm}^2 \tag{16}$$

$$\phi_{A(B)} = e^{-\alpha \bar{\boldsymbol{r}}_{1(3)}^2} \quad , \tag{17}$$

$$\mathcal{A} = \mathbb{1} - \hat{P}_{13} - \hat{P}_{24} + \hat{P}_{13}\hat{P}_{24} \quad , \tag{18}$$

$$\mathcal{V} = C_0(\Lambda) \sum_{(i,j)\in X} e^{-\frac{\Lambda^2}{4}(\boldsymbol{r}_i-\boldsymbol{r}_j)^2} \quad , \quad X = \{(13),(24)\} \quad ; \tag{19}$$

₄₆ The three-dimensional incarnation (2) which follows reads

$$(\hat{T} - E)\ \chi(\boldsymbol{r}) + \mathcal{V}^{(1)}(\boldsymbol{r})\ \chi(\boldsymbol{r}) + \int d^{(3)}\boldsymbol{r}'\ \mathcal{V}^{(2)}(\boldsymbol{r},\boldsymbol{r}',E)\ \chi(\boldsymbol{r}') = 0 \tag{20}$$

with a *local* potential which receives contributions from the identity and the complete particle exchange

$$\mathcal{V}^{(1)}(\boldsymbol{r}) = 2 \cdot C_0(\lambda) \cdot \left(\frac{2\alpha}{2\alpha+\lambda}\right)^{3/2} \cdot e^{-\frac{2\alpha\lambda}{2\alpha+\lambda}\boldsymbol{r}^2} \tag{21}$$

and a *non-local*, energy-dependent potential feeding from the kinetic and potential acting on single, odd exchanges of
a single atom between the clusters

$$\mathcal{V}^{(2)}(\boldsymbol{r},\boldsymbol{r}',E) = 8\ \alpha^{3/2} \cdot e^{-\alpha\boldsymbol{r}'^2} \cdot \left[\frac{\hbar^2}{2\mu}\ (4\alpha^2\boldsymbol{r}^2 - 2\alpha) \cdot e^{-\alpha\boldsymbol{r}^2} + E \cdot e^{-\alpha\boldsymbol{r}^2} - 2\ C_0(\lambda) \cdot \left(\frac{2\alpha}{2\alpha+\lambda}\right)^{3/2} \cdot e^{-\alpha\cdot\frac{2\alpha+3\lambda}{2\alpha+\lambda}\boldsymbol{r}^2}\right] \quad . \tag{22}$$

₄₇ It is in order to consider the following limits:

₄₈ • $\lambda \gg \alpha$

₄₉ • $\int d^{(3)}\boldsymbol{r}'\ \mathcal{V}^{(2)}(\boldsymbol{r},\boldsymbol{r}',E)\ \chi(\boldsymbol{r}') \overset{E\to 0}{\approx} \chi(\boldsymbol{r}) \cdot v^{(2)}(\boldsymbol{r}) \cdot \int d^{(3)}\boldsymbol{r}'\ v^{(2)}(\boldsymbol{r}')$.

₅₀ A comparison between the ensuing local, zero-range approximation

$$\mathcal{V}^{(0)}(\boldsymbol{r}) = \frac{\hbar^2}{2\mu}\ (4\alpha^2\boldsymbol{r}^2 - 2\alpha) \cdot 8\ \pi^{3/2} \cdot e^{-\alpha\boldsymbol{r}^2} + C_0(\lambda) \cdot \left(\frac{2\alpha}{2\alpha+\lambda}\right)^{3/2} \cdot \left(2\ e^{-2\alpha\boldsymbol{r}^2} - 16\pi^{3/2}\ e^{-3\alpha\boldsymbol{r}^2}\right) \tag{23}$$

₅₁ and the full RGM potential will enable us to quantify and trace the effect of the particle statistics.
₅₂ ECCE the following:

₅₃ • As the non-local potential factorizes, there is no mixing of partial waves and (20) applies to each partial wave

$$\left(-\frac{\hbar^2}{2\mu}\left(\partial_r^2 - \frac{l(l+1)}{r^2}\right) - E\right)\ \chi_l(r) + \mathcal{V}^{(1)}(r)\ \chi_l(r) + \int dr'\ (4\pi\ rr')\ \mathcal{V}^{(2)}(r,r',E)\ \chi_l(r') = 0 \tag{24}$$

₅₄ with a strictly local angular momentum barrier and a factor of 4π which stems from the two independent angular
₅₅ integration averages of $\chi_l(r)$ and $\chi_l(r')$. We used $\chi(\boldsymbol{r}) = r^{-1}\sum_{lm}\chi_l(r)Y_{lm}(\hat{\boldsymbol{r}})$, and projected "from the left"
₅₆ with $r \int d^{(2)}\hat{\boldsymbol{r}}\ Y_{l'm'}^*(\hat{\boldsymbol{r}})$.

₅₇ • Lorenzo, $\lambda = \frac{\Lambda^2}{4}$ and hence the pre-factor of the second term runs $\propto \Lambda^{-1}$ in EFT($\not{\pi}$) . Therefore, For $\Lambda \to \infty$,
₅₈ a model-independent interaction remains which encodes microscopic dimer characteristics via α.

e. *Example: 5-body system* In the following, we analyse features of the effective interaction for the specific case of four internal degrees of freedom and a system of five particles with identical masses. With the numerical values as given in table **??**, this example pertains to nuclear physics as described in leading order with the pionless effective field theory.

I. APPENDIX:

The normalized radial wave function corresponding to the state (nl) in a *three-dimensional isotropic oscillator potential* has the form

$$
\begin{aligned}
\phi_{nl}(r) &= C_{nl}\; e^{-\frac{\alpha^2}{2}r^2}\; r^l\; F\left[1-n, l+\frac{3}{2};\alpha^2 r^2\right]\\
&= C_{nl}\; e^{-\frac{\alpha^2}{2}r^2}\; r^l\; \left(1 + \frac{(1-n)}{(l+\frac{3}{2})}\cdot\frac{\alpha^2 r^2}{1!} + \frac{(1-n)(2-n)}{(l+\frac{3}{2})(l+\frac{5}{2})}\cdot\frac{(\alpha^2 r^2)^2}{2!} + \frac{(1-n)(2-n)(3-n)}{(l+\frac{3}{2})(l+\frac{5}{2})(l+\frac{7}{2})}\cdot\frac{(\alpha^2 r^2)^3}{3!} + \dots\right)\\
&\stackrel{l=0}{=} C_n\; e^{-\frac{\alpha^2}{2}r^2}\; \left(1 + \frac{(1-n)}{(\frac{3}{2})}\cdot\frac{\alpha^2 r^2}{1!} + \frac{(1-n)(2-n)}{(\frac{3}{2})(\frac{5}{2})}\cdot\frac{(\alpha^2 r^2)^2}{2!} + \frac{(1-n)(2-n)(3-n)}{(\frac{3}{2})(\frac{5}{2})(\frac{7}{2})}\cdot\frac{(\alpha^2 r^2)^3}{3!} + \dots\right)\\
&= e^{-\frac{\alpha^2}{2}r^2}\sum_{i=1}^{n}(-)^{i+1}\; r^{2(i-1)}
\end{aligned}
$$

with $n = 1, 2, 3, \dots$, $l \geq 0$, and normalization $C_{nl} = \frac{1}{\Gamma(l+3/2)}\sqrt{\frac{2\Gamma(1+n+1/2)}{\Gamma(n)}}\sqrt{(M\omega/\hbar)^{l+3/2}}$. The part of the function in brackets is > 0 at $r = 0$, and intersects the x axis $n-1$ times before diverging with $(-)^{n+1}\; r^{2(n-1)}$.

Systems with more particles than accessible internal states require a spatial state with mixed symmetry, *i.e.*, at least one particle has to reside in a state which is different from the one the others are in, *e.g.*, A core particles in a $n = l = 0$ state, and one particle in an $n \neq 0$ but still $l = 0$ state. Matrix elements of contact interaction between such configurations are zero, and we shall need to know whether the same is true for a one-parameter, spherically symmetric, finite-range representation of the contact, $\lim_{\Lambda\to\infty} g_\Lambda(r) = \delta(r)$.

II. APPENDIX: ON THE MICROSCOPIC INTERACTION STRENGTH

In this work, the interaction between atoms is assumed to be represented by a two- and a three-body contact interaction which are renormalized to the atom-atom and atom-atom-atom amplitudes, respectively, at an energy which is small relative to the distance between those three singular structures in the three-atom amplitude with the lowest energies *wrt.* the atom-atom-atom structure, and the fourth-closest singularity.

Specifically, this choice determines the dependence of the interaction strengths $C_0(\Lambda)$ and $D_1(\Lambda)$ on the cutoff, which is, the range of the potential operators. Linear combinations of these strengths characterize the macroscopic interaction along with the corresponding Gaussian exponents. The dependence of a two-fragment amplitude on the RG parameter Λ is thus given. In general, it is reasonable to infer from the divergence of the strength of an interaction in the course of a symmetry transformation to infinite attraction, while simultaneously its range remains finite, an ill-defined and thus useless theory. On the other hand, no meaning can come from a divergence of a theory that represents an infinite repulsion with infinite range. All other cases are candidates for theories with predictable power for macroscopic quantities based on the dynamics of their microscopic structure.

After these general consideration, we shall apply the rational to the case where mass and threshold scales are semblances of the nuclear regime.

III. APPENDIX: THE CORE WAVE FUNCTION

I assume that a spin-independent zero-range interaction renormalized to a shallow dimer and a shallow trimer implies the existence of a sequence of particle-stable bosonic A-body states with binding energies ordered as in

$$0 \approx B(2) \lesssim B(3) < B(4) < \dots < B(A_{\max}) \approx B_{\mathrm{GS}}(4)\; . \tag{25}$$

Thus, a single bound state comprises the discrete spectrum for $A < 4$, while for $A \geq 4$, a pair of states emerges with one close to the next-smaller $A+1$ threshold and the ground state relatively deep. Further I assume that the $2+1^{(A-1)}$ system emerges as a pole at the $A+1$ normal branch point which marks the onset of scattering of a single particle off the A-boson ground state. In some surrounding of this branch point, the amplitude describes either elastic scattering or a two-fragment bound state.

Our ansatz for this A-boson ground state (symmetric in space *wrt.* particle exchange) is

$$\phi_A := e^{-\frac{a}{2}\sum_{i=1}^{A}\bar{r}_i^2} = e^{-a\sum^{A-1}\bar{r}_i^2 - a\sum_{i<j}^{A-1}\bar{r}_i\cdot\bar{r}_j}\; . \tag{26}$$
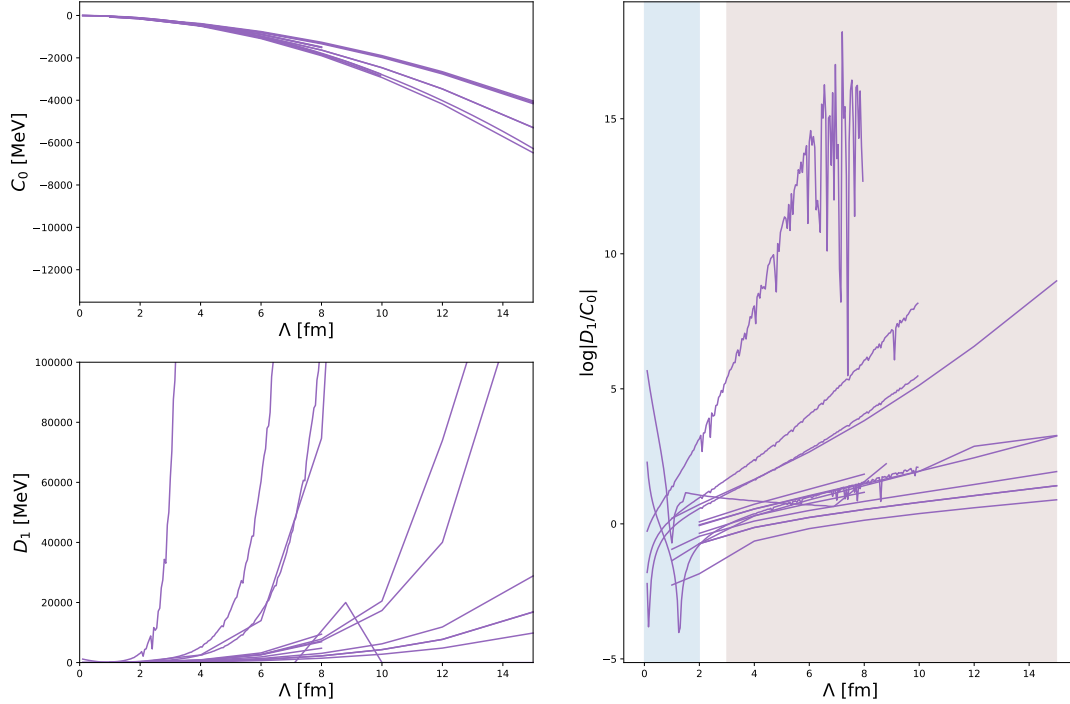
FIG. 1. Cutoff dependence of the two- and three-body interaction strengths, individually and relative to each other. The various curves. The various dependencies correspond to $B(2) \in (0, 20)$ and $B(3) \in (1.5, 54)$ for atom masses between 938 MeV and 1640 MeV. The shades roughly mark interval in which the three-body force is attractive (blue) or repulsive (brown).

From fig. II, we draw the following conclusions:

- $D_1(\Lambda) \propto e^{\kappa \Lambda}$ for $\Lambda >$ some lower limit which is related to $B(3)$ and is close to the point where the interaction strength changes sign, namely, from an attractive to a repulsive force.

- Foreseeing another bound state to enter the three-atom spectrum once the interaction strength reaches a certain magnitude at some cutoff, we expect this pattern to repeat itself if one identifies that newly found pole as the one which represents the renormalization condition for $D_1(\Lambda)$.

- For $B(2) \to 0$ and $B(3) \to 0$, *i.e.*, in the multi-resonant limit, the three-body force has a static, repulsive character. The interaction pair is "Janus-like", an always attractive two-body side and an ever repulsive three-body face.

Instead of single-particle coordinates, the usage of cluster coordinates identifies the centre of mass as the origin of a "harmonic", effective potential, in which the particles reside in their independent-particle/mean-field ground state. All observables of the system in this state depend thus on a single parameter, the (oscillator) width a. The root-mean-square radius, in particular, relates to a via

$$\mathfrak{r}^2 = \frac{\int\limits_{\mathbb{R}^{3(A-1)}} d(\bar{\boldsymbol{r}}_1, \ldots, \bar{\boldsymbol{r}}_{A\text{-}1}) \; \sum_{i=1}^{A-1} \bar{\boldsymbol{r}}_i^2 \phi_A^2}{\int\limits_{\mathbb{R}^{3(A-1)}} d(\bar{\boldsymbol{r}}_1, \ldots, \bar{\boldsymbol{r}}_{A\text{-}1}) \; \phi_A^2} \tag{27}$$

$$= \frac{3}{2} \cdot \frac{(A-1)^2}{A} \cdot a^{-1} \stackrel{A \gg 1}{=} \frac{3}{2} \cdot A \cdot a^{-1} \quad . \tag{28}$$

We assume the correlation between the radius $\mathfrak{r}$ and the ground-state wave function of the 3-nucleon system, to hold for any spatially symmetric A-boson system. However, the functional relation, $\mathfrak{r} = f[A, B(3), B(2)]$, is unknown (to the best of our knowledge).

We employ the assumption of a radius which grows almost proportional to the volume of A spheres, *i.e.*, $\propto A^{\frac{1}{3}+\delta_V}$.

7

With the parameter δ_V, deviations from the liquid-drop approximation are allowed,

$$\delta_V \begin{cases} > 0 & \text{faster than voluminous growth} \\ < 0 & \text{less than volume growth} \end{cases}$$

100 By "SVM measuring" r_0 for some A, we implicitly relate the parameters of the theory, namely, the cutoff λ, the mass
101 m_N, and the LECs/few-body renormalization conditions to a.

IV. APPENDIX: INTER-CLUSTER POTENTIAL

Consider two compound systems, whose relative motion is much slower compared with the motion of the particles within each of these fragments. Within an arbitrarily small time interval, the probability of a given particle to interact/hit/overlap with another particle is then enhanced for the partner belonging to the same compound.

$$P_{dt}(\text{intra}) \gg P_{dt}(\text{inter})$$

or

$$\#(\text{internal collisions}) \gg \#(\text{inter-cluster collisions}) \ .$$

The relative motion of particles within each cluster is then decoupled from, *one*, the relative motion *wrt.* the other cluster(s), *and two*, the internal motion in those. In turn, the internal structure affects cluster-relative motion. This reasoning underlies the single-channel resonating-group approximation and also foreshadows the non-hermitian character of the effective interaction.

$$\widehat{M}_{\mathrm{D}} = \begin{pmatrix} 4a & & \\ & 4a & (2a)_{\nabla} \\ (2a)_{\triangle} & \ddots & \\ & & 4a \end{pmatrix} \ ; \ \ \boldsymbol{\mathcal{S}}_{\mathrm{D}} = \mathbf{0} \ ; \ \ B_{\mathrm{D}} = (R - R') \tag{29}$$

Properties of the effective $2+1^{(A-1)}$ *potential* Strength factors and exponents, *i.e.*, ranges, of the effective two-body potential between an A-boson bound state and a particle which is flavour- and mass-equal to one of the bosons are listed in table **??**.

- All terms in the effective potential retain a finite range even for zero-range two- and three-body interactions ($\Lambda \to \infty$).

- The range of terms originating from the two-body interaction is $\approx 2\times$ as large as the one of the terms proportional to D_1^{Λ}.

- For $A \to \infty$, the interaction becomes local, *i.e.*, $\beta \to 0$.

- For $A \gg 1$, the terms η_1 and ζ_2 grow linearly with A consistent with the number of pairwise interactions between the orbiter and a core constituent. The terms $\eta_{2,3}$ and $\zeta_{3,4}$) increase in magnitude quadratically with A which reflects the $(A-1)(A-2)$ possible ways triplets can be selected including the orbiter and two core particles.

- The strength of the exchange term (ζ_1) is independent of A and Λ. It depends linearly on the energy and is repulsive in even, and attractive in odd partial waves ($i^l j_l(ir) \gtrless 0 \ \ \forall r$ for $\substack{\text{even} \\ \text{odd}} \ l$).

$$
\begin{aligned}
\mathfrak{v}(\boldsymbol{R},\boldsymbol{R}') =\ & C_0^\Lambda \cdot \frac{8A'(aA)^{3/2}}{\left(4aA+A'\Lambda^2\right)^{3/2}} && \cdot\, e^{-\frac{aA\Lambda^2}{4aA+A'\Lambda^2}\boldsymbol{R}^2} && \left(V_{dir}^{(2)}\right) \\[2mm]
& + D_1^\Lambda \cdot \frac{32a^3A''A'A^{3/2}}{\left(16a^2A+4a(3A-1)\Lambda^2+A''\Lambda^4\right)^{3/2}} && \cdot\, e^{-\frac{2aA\Lambda^2\left(2a+\Lambda^2\right)}{16a^2A+4a(3A-1)\Lambda^2+A''\Lambda^4}\boldsymbol{R}^2} && \left(V_{dir}^{(3_a)}\right) \\[2mm]
& + D_1^\Lambda \cdot \frac{32a^3A''A'A^{3/2}}{\left(16a^2A+8a(A-1)\Lambda^2+A''\Lambda^4\right)^{3/2}} && \cdot\, e^{-\frac{2aA\Lambda^2}{4aA+A''\Lambda^2}\boldsymbol{R}^2} && \left(V_{dir}^{(3_*)}\right)
\end{aligned}
$$

- -

$$
+ \frac{2\sqrt{2}(aA^3)^{3/2}}{\left(A'(A+1)^2\right)^{3/2}}\cdot\widehat{\mathfrak{S}}_1 \qquad \cdot\, e^{-\frac{a\left(A^3+A\right)}{2A'(A+1)^2}\boldsymbol{R}^2-\frac{2aA^2}{A'(A+1)^2}\boldsymbol{R}\cdot\boldsymbol{R}'-\frac{a\left(A^3+A\right)}{2A'(A+1)^2}\boldsymbol{R}'^2}\qquad \left(V_{Ex}^{(\mathbb{1})}\right)
$$

- -

$$
+ C_0^\Lambda \cdot \frac{8\pi^{-3/2}(A+1)^{-3}A'(aA)^{9/2}}{\left(4a^2A'+aA''\Lambda^2\right)^{3/2}}
$$
$$
\cdot\, e^{-\frac{aA\left(4a\left(A^2+1\right)+\left(3A^2+A+2\right)\Lambda^2\right)}{2(A+1)^2\left(4aA'+A''\Lambda^2\right)}\boldsymbol{R}^2}
$$
$$
\cdot\, e^{-\frac{4aA^2\left(2a+\Lambda^2\right)}{(A+1)^2\left(4aA'+A''\Lambda^2\right)}\boldsymbol{R}\cdot\boldsymbol{R}'}
$$
$$
\cdot\, e^{-\frac{aA\left(4a\left(A^2+1\right)+\left(A^2-A+2\right)\Lambda^2\right)}{2(A+1)^2\left(4aA'+A''\Lambda^2\right)}\boldsymbol{R}'^2}\qquad\left(V_{Ex}^{(2)}\right)
$$

$$
+ D_1^\Lambda \cdot \frac{32\pi^{-\frac{3}{2}}(A+1)^{-3}A''A'(aA)^{9/2}}{\left(16a^2A'+4a(3A-4)\Lambda^2+A'''\Lambda^4\right)^{3/2}}
$$
$$
\cdot\, e^{-\frac{aA\left(16a^2\left(A^2+1\right)+4a\left(5A^2+A+4\right)\Lambda^2+\left(5A^2+2A+3\right)\Lambda^4\right)}{2(A+1)^2\left(16a^2A'+4a(3A-4)\Lambda^2+A'''\Lambda^4\right)}\boldsymbol{R}^2}
$$
$$
\cdot\, e^{-\frac{2aA^2\left(16a^2+16a\Lambda^2+3\Lambda^4\right)}{(A+1)^2\left(16a^2A'+4a(3A-4)\Lambda^2+A'''\Lambda^4\right)}\boldsymbol{R}\cdot\boldsymbol{R}'}
$$
$$
\cdot\, e^{-\frac{aA\left(16a^2\left(A^2+1\right)+4a\left(3A^2-A+4\right)\Lambda^2+\left(A^2-2A+3\right)\Lambda^4\right)}{2(A+1)^2\left(16a^2A'+4a(3A-4)\Lambda^2+A'''\Lambda^4\right)}\boldsymbol{R}'^2}\qquad\left(V_{Ex}^{(3_a)}\right)
$$

$$
+ D_1^\Lambda \cdot \frac{32\pi^{-\frac{3}{2}}(A+1)^{-3}A''A'(aA)^{9/2}}{\left(16a^2A'+4a(2A-4)\Lambda^2+A'''\Lambda^4\right)^{3/2}}
$$
$$
\cdot\, e^{-\frac{aA\left(4a\left(A^2+1\right)+\left(5A^2+2A+3\right)\Lambda^2\right)}{2(A+1)^2\left(4aA'+A'''\Lambda^2\right)}\boldsymbol{R}^2}
$$
$$
\cdot\, e^{-\frac{2aA^2\left(4a+3\Lambda^2\right)}{(A+1)^2\left(4aA'+A'''\Lambda^2\right)}\boldsymbol{R}\cdot\boldsymbol{R}'}
$$
$$
\cdot\, e^{-\frac{aA\left(4a\left(A^2+1\right)+\left(A^2-2A+3\right)\Lambda^2\right)}{2(A+1)^2\left(4aA'+A'''\Lambda^2\right)}\boldsymbol{R}'^2}\qquad\left(V_{Ex}^{(3_*)}\right)
$$

The strengths of the exchange-interaction terms for $A\gg 1$ and/or $\Lambda\gg 1\,\mathrm{fm}^{-1}$ is then related to the corresponding direct-interaction strength via

$$
\zeta_{n+1} = \eta_n \cdot \left(\frac{A}{A+1}\right)^3\left(\frac{a}{\pi}\right)^{3/2} \quad . \tag{30}
$$

The fraction $\left(\frac{a}{\pi}\right)^{3/2}$ is the inverse of an integration of the non-local terms assuming a constant wave function (exponents scale with a which produces an $\sqrt{\pi/a}$ upon integration, and the spherical Bessel functions provide the remaining a^{-1}).

In order to study the zero-range limit and the related renormalization-group invariance, the large Λ behaviour is of interest. In this limit, the potential scales as

$$\lim_{\Lambda \to \infty} \mathfrak{v}(\boldsymbol{R}, \boldsymbol{R}') = \quad \mathcal{O}(A) \cdot \frac{C_0^\Lambda}{\Lambda^3} \cdot a^{\frac{3}{2}} \cdot e^{-a\boldsymbol{R}^2} \qquad\qquad\qquad + 2 \cdot \mathcal{O}(A^2) \cdot \frac{D_1^\Lambda}{\Lambda^6} \cdot a^3 \cdot e^{-2a\boldsymbol{R}^2}$$

$$+ \mathcal{O}(A) \cdot \frac{C_0^\Lambda}{\Lambda^3} \cdot a^3 \cdot e^{-\frac{3}{2}a\boldsymbol{R}^2 - \frac{4a}{\mathcal{O}(A)}\boldsymbol{R}\cdot\boldsymbol{R}' - \frac{3}{2}a\boldsymbol{R}'^2} \qquad + 2 \cdot \mathcal{O}(A^2) \cdot \frac{D_1^\Lambda}{\Lambda^6} \cdot a^{\frac{9}{2}} \cdot e^{-\frac{5}{2}a\boldsymbol{R}^2 - \frac{6a}{\mathcal{O}(A)}\boldsymbol{R}\cdot\boldsymbol{R}' - \frac{5}{2}a\boldsymbol{R}'^2}$$

$$+ \mathcal{O}(1) \cdot a^{\frac{3}{2}} \cdot e^{-\frac{a}{2}\boldsymbol{R}^2 - 2a\boldsymbol{R}\cdot\boldsymbol{R}' - \frac{a}{2}\boldsymbol{R}'^2} \quad ,$$

and terms were organized their origin from pair or triplet interactions. The third-row term stems from the norm-exchange kernel. This skeleton of the potential is now fed into the partial-wave projected RGM equation (13) to yield

$$\int \left\{ \frac{\hbar^2}{2\mu} \left[-\partial_R^2 \left(\mathbb{1} + (\mathfrak{o}_E \leftrightarrow \mathfrak{o}_\mu) \right) + \frac{l(l+1)}{R^2} \left(\mathbb{1} + (\mathfrak{o}_E \leftrightarrow \mathfrak{o}_L) \right) \right] \phi_{lm}(R') \right. \tag{31a}$$

$$- E \left(\delta(R - R') + (-)^{l+1} \mathfrak{o}_E(1) \left(\frac{a}{\pi} \right)^{3/2} e^{+\frac{1}{2}\mathfrak{o}_E(aA^{-1})RR' - \frac{1}{2}\mathfrak{o}_E(a)\boldsymbol{R}^2 - \frac{1}{2}\mathfrak{o}_E(a)\boldsymbol{R}'^2} \right) \tag{31b}$$

$$+ \mathfrak{o}_2(A) \cdot \frac{C_0^\Lambda}{\Lambda^3} \cdot a^{\frac{3}{2}} \cdot e^{-\mathfrak{o}_2(a)\boldsymbol{R}^2} \left(\delta(R - R') + (-)^{l+1} \mathfrak{o}_2(1) \left(\frac{a}{\pi} \right)^{3/2} e^{+\mathfrak{o}_2(aA^{-1})RR' - \mathfrak{o}_2(a)\boldsymbol{R}'^2} \right) \tag{31c}$$

$$\left. + 2 \cdot \mathfrak{o}_3(A^2) \cdot \frac{D_1^\Lambda}{\Lambda^6} \cdot a^3 \cdot e^{-2\mathfrak{o}_3(a)\boldsymbol{R}^2} \left(\delta(R - R') + (-)^{l+1} \mathfrak{o}_3(1) \left(\frac{a}{\pi} \right)^{3/2} e^{+2\mathfrak{o}_3(aA^{-1})RR' - 2\mathfrak{o}_3(a)\boldsymbol{R}'^2} \right) \right\} \phi_{lm}(R') dR' \tag{31d}$$

$$= 0 \quad .$$

The first and second row of this equation demonstrate the effect of the antisymmetrization on the single-particle characteristics of the system which is solely the reduced mass. For even partial waves, the exchange of the particle amounts to an increased mass if the particle is close to the core, while for a large separation the original mass dictates the free propagation. The distance over which the mass is significantly enlarged is set by the core size a in the exponent of (31b). The mass/kinetic-energy correction due to exchange is thus characterized repulsive or attractive solely by the partial wave (only one single permutation comprises the antisymmetrization) with strength and range increasing with the size of the core.

The exchange has qualitatively the same effect on the terms associated with the two- and three-body contact interactions. Corrections to both (31c) and (31d) increase (odd) or decrease (even) the interaction strength without changing its attractive or repulsive character. Exchange effects do not turn an attractive interaction repulsive or vice versa. A potential destabilization is thus driven by a weakening of an otherwise sufficiently attractive direct interaction in combination with a genuine but interaction-independent repulsion as emergent from the kinetic part of the system. This insight in combination with the strengths of the interaction being much larger in magnitude for $\lim_{\Lambda \to \infty}$ compared with the kinetic-energy factors justify our qualitative conjectures in the discussion of fig. **??** which were based on the local approximation.

[1] John A. Wheeler. On the Mathematical Description of Light Nuclei by the Method of Resonating Group Structure. *Phys. Rev.*, 52:1107–1122, 1937.

[2] K. Wildermuth and Y. C. Tang. *A Unified Theory of the Nucleus*. Vieweg+Teubner Verlag, Wiesbaden, 1977.

[3] H. Bethe, R. Peierls, and Douglas Rayner Hartree. Quantum theory of the diplon. *Proceedings of the Royal Society of London. Series A - Mathematical and Physical Sciences*, 148(863):146–156, 1935.

[4] A. R. EDMONDS. *Angular Momentum in Quantum Mechanics*. Princeton University Press, 1985.

[5] D. S. Petrov, C. Salomon, and G. V. Shlyapnikov. Weakly bound dimers of fermionic atoms. *Phys. Rev. Lett.*, 93:090404, Aug 2004.